JOURNAL OF MATERIALS SCIENCE: MATERIALS IN MEDICINE 7 (1996) 457–463

Synthesis, X-ray diffraction and solid-state ^{31}P magic angle spinning NMR study of α-tricalcium orthophosphate

M. BOHNER, J. LEMAÎTRE
Laboratoire de Technologie des Poudres, Ecole Polytechnique Fédérale de Lausanne, MX-Ecublens, CH-1015 Lausanne, Switzerland

A. P. LEGRAND, J.-B. d'ESPINOSE de la CAILLERIE, P. BELGRAND
Laboratoire de Physique Quantique, CNRS URA 1428, ESPCI, 10 rue Vauquelin, F-75231 Paris CEDEX 05, France

The effects of synthesis conditions on the quantitative preparation of α-tricalcium phosphate (α-TCP) have been investigated. The following parameters of the synthesis were considered: nature of the starting material – Ca-deficient hydroxyapatite, DAP, versus hydroxyapatite-anhydrous dicalcium phosphate mixtures (HAP-DCPA); Ca/P atomic ratio of the mixture, calcination temperature and time, and cooling rate. The yield and crystallinity of the final product have been estimated using X-ray diffraction (XRD) and solid state ^{31}P magic angle spinning NMR (MAS-NMR) techniques. The results show that pure, well-crystallized α-TCP powders exhibiting nearly ideal MAS-NMR spectra, can be obtained by reactive sintering of HAP-DCPA (Ca/P = 1.50...1.52) mixtures, at 1400 °C for 8 h. The broadening of MAS-NMR spectra can be used as an indicator of structural order in the final product. The α-TCP yield with DAP was always less than 50%.

1. Introduction

Since the early discovery of the similarity between HAP and the mineral fraction of bone, interest in calcium orthophosphates has been increasing in the field of biomaterials. The biomaterial community is not only interested in understanding their role in bone and tooth mineralization, but also in their use as bone replacement materials [1]. An extensive review of the general chemistry of calcium orthophosphates has been published recently by Elliott [2]. Tricalcium phosphate in its low-temperature allotropic form (β-TCP) is generally considered as a resorbable bioceramic material, although its resorbability depends to a large extent on the density and pore size distribution of the ceramic body [3].

Compared to the β polymorph, α-TCP has a lower density and a higher free energy of formation [4] and is therefore expected to be more reactive: thus, Ando [5] has shown that the solubility of TCP in ammonium citrate solutions increases considerably upon β → α conversion. Monma [6] has shown that α-TCP hydrolyses readily in water at 60–80 °C into a Ca-deficient HAP, whereas β-TCP is almost inert in the same conditions. On another hand, β-TCP is being used in the development of resorbable calcium phosphate hydraulic cements [7, 8]. Bohner [9] has shown recently that the setting rate of these cements increases when α-TCP is substituted for β-TCP in the material. It can thus be expected that resorbable bioceramics based on α-TCP would also exhibit higher resorption rates.

The standard preparation method of α- and β-TCP consists in mixing carefully stoichiometric amounts of $CaHPO_4$ (DCPA) and $CaCO_3$, and applying the appropriate heat treatment: thus Mathew *et al.* [10] prepared pure α-TCP for crystallographic studies by heating pellets of stoichiometric amounts of finely ground $CaHPO_4$ and $CaCO_3$, mixed with 1 wt % cornstarch and a few drops of distilled water; the pellets were kept at 1400 °C for 2 days, and cooled down to ambient temperature; pure α-TCP was prepared likewise by Dickens *et al.*, except that the pellets were tempered at 1100 ± 10 °C for 1 week prior to cooling [11].

Other preparations based on different raw materials have been attempted, showing that the exact TCP polymorph obtained can depend strongly on the origin of the raw material used for the synthesis, even though the same heating treatment is applied. Thus, pure α, pure β, or α + β TCP mixtures were obtained by Bredig *et al.* [12] upon tempering at 1000 °C for 2–4 h two different calcium phosphate samples heated at 1300 °C (presumably Ca-deficient apatites with Ca/P = 1.50). The thermal treatments of precipitated tricalcium phosphates also leads to contradictory results, α-TCP appearing in some cases well below the normal α–β transition temperature. Thus, according to Eanes [13], and Kanazawa *et al.* [14], amorphous

tricalcium phosphate prepared by aqueous precipitation transforms first into α-TCP upon heating at 600–800 °C, β-TCP being observed above 850 °C, whereas Mortier *et al.* found that stoichiometric mixtures of HAP and DCPA [15], as well as Ca-deficient HAP (Ca/P = 1.50) [16] transform directly into β-TCP in the 700–1000 °C range.

Thermodynamic and kinetic effects may explain the discrepancies observed: departures from the ideal Ca/P ratio, and impurities can affect the equilibrium temperature of the α–β transition, and/or the rate of the α–β inversion. In their reference study on the $CaO–P_2O_5$ equilibrium phase diagram, Welch and Gutt [17] established the equilibrium α–β inversion temperature of pure stoichiometric TCP to be 1125 °C. Although pure α-TCP could be easily isolated by quenching the stoichiometric mixture from 1200–1250 °C, this procedure was not satisfactory for TCP samples with $1.37 < Ca/P < 1.50$ (TCP solid-solution range), whereby only α–β mixtures could be obtained. These authors ascribe this result to an acceleration of the α–β inversion in the presence of $\alpha\text{-}Ca_2P_2O_7$, and recognize that "precise location of the α–β inversion in $2Ca_2O \cdot P_2O_5$ and $3CaO \cdot P_2O_5$ for mixtures lying between these compositions was not attempted".

Some impurities, such as SiO_2 and MgO, also affect considerably the α–β inversion temperature: thus, according to Trömel *et al.* [18], less than 1 wt % SiO_2 can decrease the α–β inversion temperature below 1050 °C; more accurate results of Nurse *et al.* [19] point to a decrease of the inversion temperature below 500 °C with only 0.4% SiO_2. Likewise, Ando [20] has shown that less than 2 wt % MgO was sufficient to raise the α–β conversion temperature of TCP to 1500 °C.

The crystal structure of α-TCP has been determined by Mathew *et al.* [10]: α-TCP crystallizes in the monoclinic space group P21/*a*, with cell parameters $a = 1.2887_2$, $b = 2.7280_4$, $c = 1.5219_2$ nm, and $\beta = 126.20_1°$ at 25 °C, with $Z = 24$; the calculated density is 2.863 g/cm^3. An approximate prominent subcell exists with $b'' = b/3$. The structure is closely related to the mineral glaserite $K_3Na(SO_4)_2$, and contains 48 different phosphorus atoms (16 per subcell), so that the ^{31}P MAS-NMR spectrum of α-TCP is expected to resolve into a maximum of 16 components.

The crystal structure of β-TCP has been determined by Dickens *et al.* [11]: β-TCP crystallizes in the rhombohedral space group R3c with cell parameters $a = 1.0439_1$ and $c = 3.7375_6$ nm (hexagonal setting) at 25 °C, with 21 formula units per hexagonal unit cell; the calculated density is 3.067 g/cm^3. The structure contains only three different phosphorus environments, which have been effectively resolved by MAS-NMR [21].

The purpose of the present work is to investigate the effects of some preparation parameters on the formation of α-TCP, such as calcination conditions, Ca/P and nature of the starting material (HAP-DCPA mixtures, or Ca-deficient HAP), and to test the use of ^{31}P MAS-NMR for characterizing the purity and state of crystallization of the obtained samples.

2. Experimental methods

2.1. Experimental designs

In order to address the effects of several factors simultaneously, the methodology of factorial experiments has been used systematically in this study [22]. The results have been analysed using the ANOVA technique.

First series of experiments: The five factors specified in Table I were tested in a two-level multi-factorial design, in order to assess their effect on the α-TCP yield of samples prepared by reactive sintering of HAP-DCPA mixtures.

One replicate of the full experimental design requires 32 ($= 2^5$) experiments. In order to reduce the total number of experiments down to 16 ($= 2^{5-1}$), it was decided to perform only one half of the full experimental design, selecting the experiments so as to confound the effect of factor E with the high-order interaction between the four remaining factors (ABCD). The resulting design is summarized in Table II.

The complete list of experiments to be performed is summarized in Table II.

For the purpose of comparison, samples were prepared from DAP (Ca/P atomic ratio = 1.50) according to the same heating cycles as in Table II. In total, eight samples were prepared, corresponding to a 2^3 factorial design involving only the factors A, B and D of Table I. The heating conditions thus applied correspond to experiments 5 to 8, and 13 to 16 in Table II.

Second series of experiments: The three factors specified in Table III were tested at two levels, in order to assess their effect on the final α-TCP yield of samples prepared by reactive sintering of HAP-DCP mixtures. The complete list of experiments is summarized in Table IV.

2.2. Preparation of the specimens

2.2.1. Specimens prepared by reactive sintering of HAP-DCPA mixtures

First experimental design: Four batches of 80 g were prepared, corresponding to the different combinations of Ca/P ratios (1.45–1.50) and homogenization times (2–4 h). Thus, each batch was prepared by mixing the appropriate proportions of hydroxyapatite (HAP Merck, cat. n° 2194, lot n° 535K973044), and anhydrous dicalcium phosphate (DCPA Merck, cat. n° 2144, lot n° 535K973044), followed by homogenization in a 500 ml PEBD bottle containing five alumina balls (18 g), with a Turbula mixer running at 42 rpm for the specified time. Each batch was then divided in four samples of 20 g, in order to dispose of the 16 samples necessary to perform the planned thermal treatments.

TABLE I First experimental design: factor definitions

Factor	Definition	Low level	High level
A	Dwell time	2 h	4 h
B	Dwell temperature	1300 °C	1400 °C
C	Ca/P ratio	1.47	1.50
D	Cooling rate	300 °C/h	600 °C/h
E	*Mixing time*	1 *h*	2 *h*

TABLE II First experimental design: list of experiments

Test number	Treatment	Dwell time (h)	Dwell temperature (°C)	Ca/P ratio	Cooling rate (°C/h)	*Mixing time (h)*
1	(e)	2	1300	1.47	300	*2*
2	a	4	1300	1.47	300	*1*
3	b	2	1400	1.47	300	*1*
4	ab(e)	4	1400	1.47	300	*2*
5	c	2	1300	1.50	300	*1*
6	ac(e)	4	1300	1.50	300	*2*
7	bc(e)	2	1400	1.50	300	*2*
8	abc	4	1400	1.50	300	*1*
9	d	2	1300	1.47	600	*1*
10	ad(e)	4	1300	1.47	600	*2*
11	bd(e)	2	1400	1.47	600	*2*
12	abd	4	1400	1.47	600	*1*
13	cd(e)	2	1300	1.50	600	*2*
14	acd	4	1300	1.50	600	*1*
15	bcd	2	1400	1.50	600	*1*
16	abcd(e)	4	1400	1.50	600	*2*

TABLE III Second experimental design: factor definitions

Factor	Definition	Low level	High level
A	Dwell time	4 h	8 h
B	Dwell temperature	1400 °C	1450 °C
C	Ca/P ratio	1.50	1.52

TABLE IV Second experimental design: list of experiments

Test number	Treatment	Dwell time (h)	Dwell temperature (°C)	Ca/P ratio
1	'1'	4	1400	1.50
2	a	8	1400	1.50
3	b	4	1450	1.50
4	ab	8	1450	1.50
5	c	4	1400	1.52
6	ac	8	1400	1.52
7	bc	4	1450	1.52
8	abc	8	1450	1.52

Second experimental design: Two batches of 80 g were prepared by mixing the appropriate quantities of HAP and DCPA, corresponding to the two selected Ca/P ratios (1.50 and 1.52). The batches were homogenized for 2 h in the Turbula mixer, in the same conditions as above.

2.2.2. Specimens prepared by calcination of DAP

The raw material used was a Ca-deficient hydroxyapatite (DAP, atomic ratio Ca/P = 1.50, Merck, cat. n° 2143, lot n° 532K837143). Eight samples 20 g each were submitted to the heating cycles specified in the experimental design, without any further pretreatment.

2.3. Thermal treatments

First experimental design: The thermal cycles were performed in synthetic dry air in an atmosphere-controlled furnace (Linn 1800-G chamber furnace, 30 l capacity, heating rate 300 °C/h up to the desired temperature, gas flow 3 l/min, cooling rate 300 or 600 °C/h). Each 20 g specimen was placed in an alumina crucible ($\emptyset_{int} \times \emptyset_{ext} \times$ height = 35 × 40 × 88 mm). In order to prevent any experimental bias caused by a possible lack of temperature uniformity in the furnace, the positions in the furnace of the three crucibles (one for each HAP-DCP mixture and one for DAP) were ascribed by tossing.

Second experimental design: Prior to the final calcination treatment, the batches were prefired at 1000 °C (same conditions as above, cooling rate 300 °C/h). After cooling, they were homogenized by grinding until all the powder passed through a 250 μm sieve. For the final calcination treatment, the samples (20 g each) were placed in two alumina crucibles ($\emptyset_{int} \times \emptyset_{ext} \times$ height = 94 × 104 × 100 mm). The calcination treatments were performed in the same conditions as above, with a fixed cooling rate of 600 °C/h.

2.4. Characterization techniques

2.4.1. X-ray diffraction

The specimens were analyzed by X-ray diffraction with a Siemens Kristalloflex 805 diffractometer, in the following conditions: CuK_α radiation (source conditions: 40 kV, 35 mA), step scanning 0.04° 2θ/step, 4 s accumulation per step. The α-TCP yield was estimated as $\log(I_\alpha/I_\beta)$, where I_α is the intensity of the main diffraction peak of α-TCP, and I_β that of the 55% peak of β-TCP (d_α = 0.291 nm, d_β = 0.288 nm).

2.4.2. MAS-NMR

The ^{31}P spectra were obtained on a ASX500 spectrometer (Burker Spectrospin, magnetic field, 11.7 T,

frequency 202.4 MHz). After optimization, the acquisition parameters were set as follows: single 2.7 μs impulsion with recycle time of 120 s and eight acquisition. The recycle delay is large compared to the spin-lattice relaxation time. Magic angle spinning (MAS) spectra were obtained on 150 mg dry powder samples tightly packed into double-bearing-type rotors, spun at 10 KHz.

Chemical shifts were referred to 85% H_3PO_4 aqueous solution. No line broadening was applied prior to Fourier transform.

3. Results and discussion

3.1. First experimental design

3.1.1. X-ray diffraction

Samples prepared by reactive sintering. The results are summarized in Table V.

Fig. 1 presents the results, together with the regression equation deduced from their statistical analysis ($p < 0.01$ means that the risk of accepting erroneously the significance of some effect is less than 1%; X_f is the coded level of factor F: $X_f = -1$ for the lower level, $+1$ for the higher level). As shown in the figure, the four main factors A, B, C and D and several interactions between these factors affect log(α/β) significantly. Little conversion into a α-TCP is obtained with the lowest Ca/P ratio (treatments '1' to ab, and d to abd): no conversion at 1300 °C, and about 10% conversion at 1400 °C, with a slight decrease in α-TCP yield with dwell time; in this case, no effect of cooling rate (factor D) is observed. With Ca/P = 1.50 (treatments c, to abc, and cd to abcd), considerable effects of dwell time (A), dwell temperature (B) and cooling rate (D) are observed: at 1300 °C, the yield decreases slightly at longer dwell time (compare treatments c and ac, or cd and acd), while a moderate increase occurs at faster cooling rate (compare c and cd, ac and acd). At 1400 °C, longer heating and faster cooling both increase the α-TCP yield considerably: in this case the contribution of the factors is essentially additive. The best result (> 98% α-TCP) is obtained by using a mixture with Ca/P = 1.50, heating for 4 h at 1400 °C, and cooling at 600 °C/h (treatment abcd). The critical role of cooling rate is remarkable here: cooling faster will contribute to a 40% increase in α-TCP yield, but only with Ca/P = 1.50 and $T = 1400$ °C. Note in passing that the results are not affected by the mixing time (E, confounded with interaction ABCD).

Samples prepared from DAP. The results are summarized in Table V. Fig. 2 presents the results and the regression equation deduced from the statistical analysis ($p < 0.05$). Only the dwell time (A) affects the

TABLE V First experimental design: XRD estimates of α-TCP yield, expressed as log(α/β)

Test number	Treatments	log(α/β)[a]	
		Reactive sintering	DAP
1	(e)	− 1.690	−
2	a	− 1.690[b]	−
3	b	− 0.711[b]	−
4	ab(e)	− 0.974	−
5	c	− 0.575	− 0.160
6	ac(e)	− 0.845	− 0.038
7	bc(e)	− 0.899	− 0.105
8	abc	0.185	− 0.049
9	d	− 1.690[b]	−
10	ad(e)	− 1.690[b]	−
11	bd(e)	− 0.837	−
12	abd	− 1.079	−
13	cd(e)	− 0.343	− 0.213
14	acd	− 0.315	− 0.066
15	bcd	0.321	− 0.082
16	abcd(e)	1.690	− 0.094

[a] Average over five XRD measurements.
[b] Inhomogeneous, partially fused specimens.

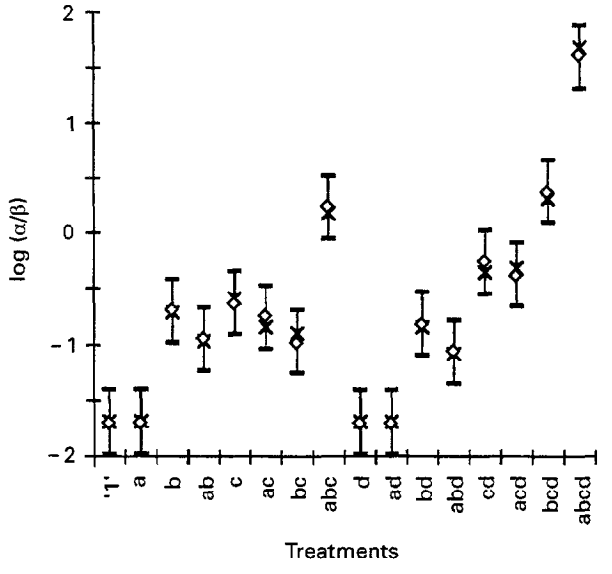

Figure 1 Reactive sintering: α-TCP yields expressed as log(α/β). (A) dwell time (2–4 h), (B) temperature (1300–1400 °C), (C) Ca/P ratio (1.47–1.50), and (D) cooling rate (300–600 °C/h). Regression equation: $\langle Y \rangle = -0.696 + 0.107X_a + 0.409X_b + 0.137X_aX_b + 0.599X_c + 0.170X_aX_c + 0.200X_aX_bX_c + 0.203X_d + 0.108X_bX_d + 0.232X_cX_d + 0.137X_bX_cX_d$ ($p < 0.01$) × Exp. ◇Adj. The bar denotes ± 3SE.

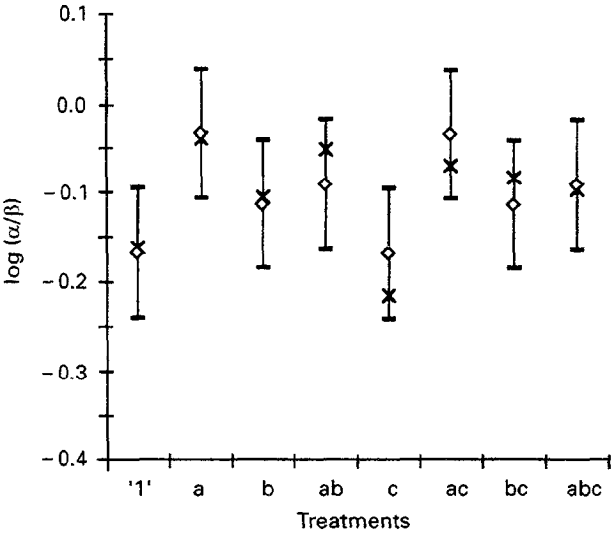

Figure 2 DAP samples: α-TCP yields expressed as log(α/β). (A) dwell time (2–4 h), (B) temperature (1300–1400 °C) and (C) cooling rate (300–600 °C/h). Regression equation $\langle Y \rangle = -0.101 + 0.039X_a - 0.028X_aX_b$ ($p < 0.05$) × Exp. ◇Adj. The bar denotes ± 3SE.

α-TCP yield significantly, although to a lesser intensity at higher temperature (AB interaction); no significant effect of cooling rate (C) is perceptible here.

The most striking fact, however, is that, although statistically significant ($p < 0.05$), the effects observed on DAP samples are small (< 5% increase in yield) compared to those observed with reactive sintering; moreover, the maximum yield obtained with DAP is below 50%. For this reason, this source of TCP has no longer been considered in further experiments.

3.1.2. MAS-NMR

A typical MAS-NMR spectrum of the series prepared from DAP (sample '1') is presented in Fig. 3a. Also shown on the same figure is the total simulated spectrum 3b, and the result of the subtraction of the α-TCP contribution 3d, which was estimated as follows: the α-TCP component (spectrum of sample bc of the second experimental design) was multiplied by a normalization coefficient (c), chosen by trial and error such as to remove any characteristic features of α-TCP from the residual spectrum 3e. The resulting spectrum 3d can be decomposed into the three characteristic components of β-TCP, hence confirming the XRD results. The decomposition of the MAS-NMR spectra of this series allowed a semi-quantitative estimate of the α-TCP yield (43 ± 5% for all specimens), in good agreement with the XRD results.

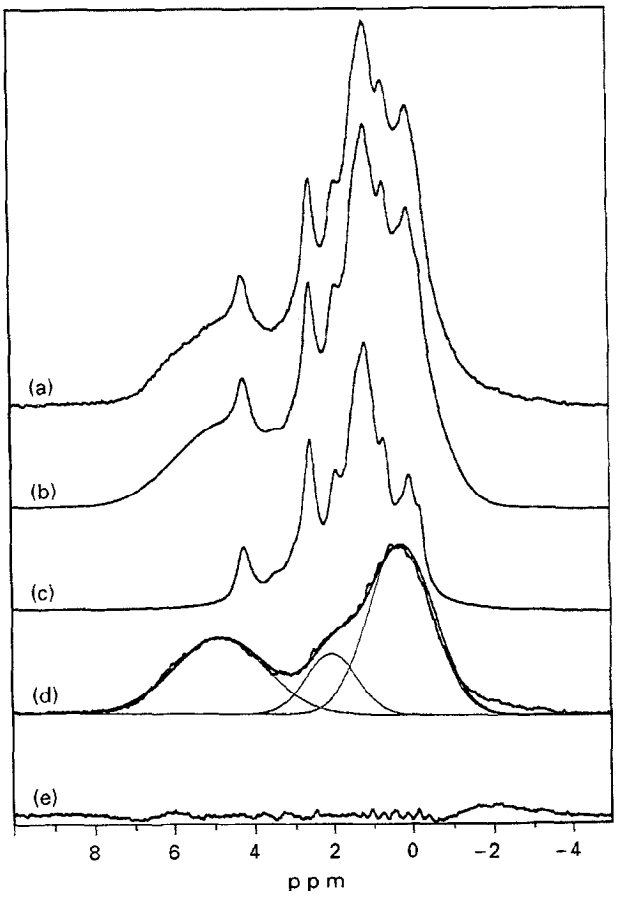

Figure 3 ^{31}P MAS-NMR spectrum of specimen '1' of the DAP series (first experimental design: (a) experimental spectrum; (b) total simulated spectrum; (c) α-TCP contribution to the experimental spectrum (see text); (d) difference (a − c), and fit to a simulated β-TCP spectrum; (e) residual.

TABLE VI Second experimental design: XRD estimates of α-TCP yield, expressed as log(α/β), and broadening of ^{31}P MAS-NMR spectra (λ)

Test number	Treatments	log(α/β)[a]	λ (ppm)
1	'1'	1.700	0.408
2	a	1.673	0.300
3	b	1.686	0.409
4	ab	1.680	0.391
5	c	1.785	0.311
6	ac	1.796	0.344
7	bc	1.731	0.304
8	abc	1.747	0.411

[a] Average over five XRD measurements.

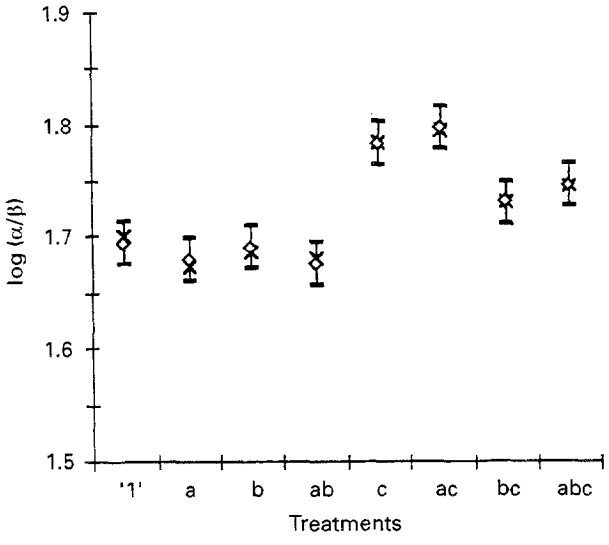

Figure 4 Reactive sintering (second experimental design): α-TCP yields expressed as log(α/β). (A) dwell time (4–8 h), (B) temperature (1400–1450 °C) and (C) Ca/P ratio (1.50–1.52). Regression equation: $\langle Y \rangle = 1.725 - 0.014X_b + 0.040X_c + 0.007X_aX_c - 0.012X_bX_c$ ($p < 0.05$). The bar denotes ± 3SE.

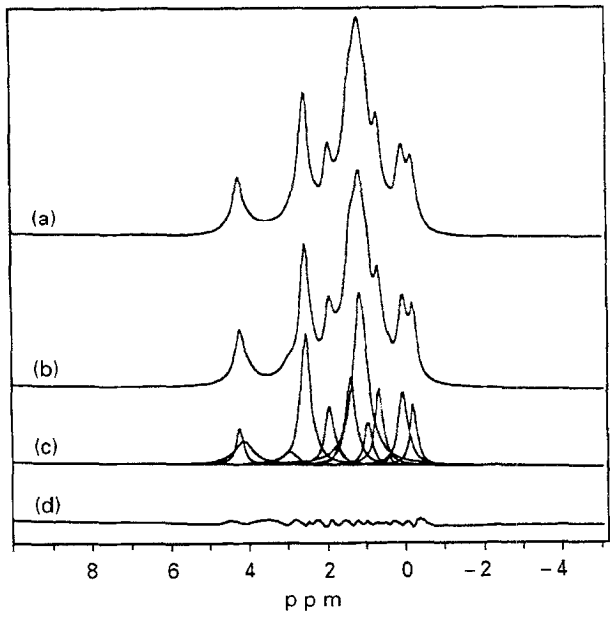

Figure 5 ^{31}P MAS-NMR spectrum of a specimen ac (reactive sintering, second experimental design): (a) experimental spectrum; (b) simulated spectrum; (c) decomposition into 15 Lorentzian components according to the theoretical α-TCP crystallographic structure, (d) residual.

3.2. Second experimental design (samples prepared by reactive sintering)

3.2.1. X-ray diffraction

The results are summarized in Table VI. Fig. 4 presents the results and the regression equation deduced from their statistical analysis ($p < 0.05$). The α-TCP yield slight increases slightly (+ 0.34%) upon increasing Ca/P. Although small, this increase is significant ($p < 0.05$). Note also that the α-TCP conversion decreases slightly at higher temperature, but only for the highest Ca/P ratio.

3.2.2. MAS-NMR

All the samples exhibit a MAS-NMR spectrum corresponding to pure α-TCP. The best resolved spectrum, that of specimen ac, can be decomposed into 15 lines (Fig. 5). Although 14 lines at maximum are observable in any of the spectra, the latter were decomposed into 15 components according to the α-TCP crystallographic model, as shown in Tables VII (line amplitudes) and VIII (line areas). The chemical shifts are identical for all the samples. The decomposition was satisfactory for all samples, showing no NMR evidence for the presence of β-TCP, in perfect agreement with XRD observations. Therefore, it was decided to test the use of the global broadening of MAS-NMR spectra as a measure of local structural disorder, for estimating the crystallinity of the samples.

The average broadening λ of a given spectrum was determined by taking the ratio of its total area over the summed amplitudes of its 15 peaks. The results are reported in Table VI.

Fig. 6 presents the results and the regression equation deduced from their statistical analysis ($p < 0.01$). The results show that λ is mainly affected by the dwell temperature (B) and the Ca/P ratio (C), both factors interacting strongly with the dwell time (A): thus, with Ca/P = 1.50 (treatments '1' to ab), λ *decreases* at longer dwell times, the effect being stronger at

TABLE VII MAS-NMR results: line amplitudes (a. u.)

Line number	Line position (ppm)	Treatments							
		'1'	a	b	ab	c	ac	bc	abc
1	−0.25 ··· −0.22	7658	9925	5304	5886	8865	9304	8139	6972
2	0.03 ··· 0.05	16425	12914	9979	10197	11093	10433	9739	14501
3	0.30 ··· 0.41	2661	1436	0	0	523	0	1133	2644
4	0.65 ··· 0.68	19070	12844	9592	10187	11512	13625	10163	18362
5	0.94 ··· 0.97	14008	6530	4639	5173	6076	9776	5636	14394
6	1.14 ··· 1.15	26015	29783	20511	20680	27530	35824	23122	20852
7	1.39 ··· 1.40	27238	14492	11161	11825	12100	15599	11713	23805
8	1.70	1602	2391	1549	741	2226	417	2151	2071
9	1.90 ··· 1.93	12878	9616	6922	7553	9538	11144	7800	11746
10	2.51 ··· 2.55	26994	22329	16664	16964	20783	24220	17565	24604
11	2.96 ··· 3.02	4640	979	784	1343	1850	1823	1698	6369
12	3.44	2292	0	0	537	358	826	0	2966
13	3.82 ··· 4.12	4989	1899	1985	975	2794	1874	3071	7616
14	4.21 ··· 4.23	7075	6422	4907	6567	6022	8206	4748	5702
15	4.66 ··· 4.69	0	4524	160	0	0	328	4524	0
	Total	173545	136084	94157	98628	121270	143399	111202	162604

TABLE VIII MAS-NMR results: line areas (a. u. ppm)

Line number	Treatments							
	'1'	a	b	ab	c	ac	bc	abc
1	1761	2084	955	1413	1862	2791	1709	1603
2	7063	3745	4291	4079	3217	3547	2824	6236
3	798	215	0	0	78	0	170	793
4	6674	2954	3261	3158	2648	4087	2541	6427
5	4483	1567	1485	1242	1458	2346	1353	4606
6	9886	12807	10051	10133	11838	15404	9943	7924
7	14709	4347	5803	6149	3630	4680	3514	12855
8	481	717	465	222	668	125	645	621
9	5022	2693	1869	2039	2003	3677	2184	4581
10	10798	6699	6999	6277	6235	7750	5270	9841
11	2459	460	415	712	870	912	798	3375
12	1146	0	0	258	122	281	0	1483
13	2943	1121	834	410	1648	675	1812	4874
14	2618	1477	1815	2430	1385	2954	1092	1597
15	0	0	302	0	0	75	0	0
Total	70841	40886	38545	38522	37662	49304	33855	66816

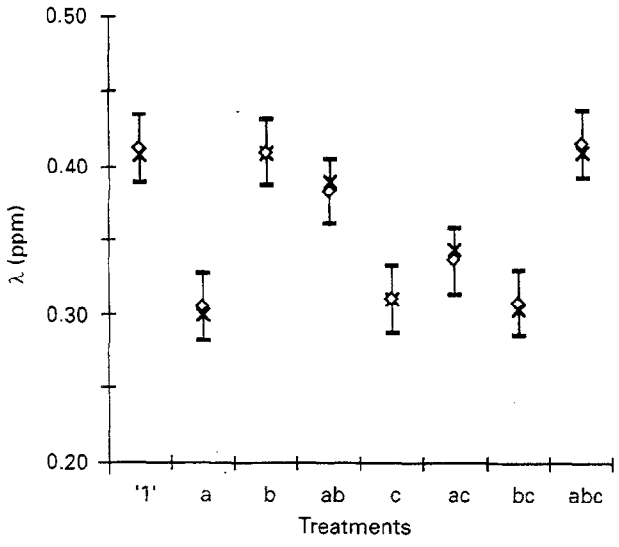

Figure 6 Broadening λ of MASS-RMN spectra. (A) dwell time (4–8 h), (B) temperature (1400–1450 °C) and (C) Ca/P ratio (1.50–1.52). Regression equation: $\langle Y \rangle = 0.360 + 0.019X_b + 0.020X_aX_b - 0.017X_c + 0.033X_aX_c$ ($p < 0.01$). The bar denotes ± 3SE.

$T = 1400\,°C$; on the other hand, with Ca/P = 1.52 (treatments c to abc), *λ increases* at longer dwell times, but now the effect is stronger at $T = 1450\,°C$.

These observations suggest that, with Ca/P = 1.50, the α-TCP is initially less ordered, possibly due to local Ca/P fluctuations; ordering of Ca and P atoms increases with time, a more ordered distribution being eventually reached at 1400 °C (treatments '1' and a). This behaviour can be explained by an increase of the material homogeneity with time: the higher final degree of disorder observed at 1450 °C probably reflects an increased entropy of the system with temperature; with Ca/P = 1.52, a higher degree of order is obtained initially, but ordering *decreases* with time, faster at higher temperatures; this latter behaviour can be tentatively ascribed to the diffusion of excess Ca into interstitial positions in the α-TCP lattice.

4. Conclusions

Pure α-TCP samples, exhibiting MAS-NMR spectra close to the one calculated from the theoretical α-TCP structure, have been obtained by reactive sintering of HAP-DCPA mixtures with an atomic ratio Ca/P = 1.50–1.52. The appropriate set of calculation conditions are: temperature = 1400–1450 °C, holding 4–8 h, cooling at 600 °C/h. The broadening of MAS-NMR spectra can be used as an indicator of structural disorder of the α-TCP crystals: the best crystallinity is obtained when heating mixtures with Ca/P = 1.50 at 1400 °C for longer than 8 h. The preparation of pure α-TCP was not possible using DAP (Ca/P = 1.50) as a precursor material: the best yield obtainable was less than 50%.

Acknowledgements

M.B. and J.L. acknowledge the financial help of EPFL, and of the Council of the Swiss Federal Schools of Technology (PPM Start program, project n° 4B3). The financial support of the company BIO-LAND (France) is also gratefully acknowledged. This work was supported by a grant from INSERM (CRE 910911). One of us (P.B.) acknowledges the BRUKER-CNRS foundation for supporting his doctoral work with a grant.

References

1. K. DE GROOT, "*Bioceramics of calcium phosphate*" (CRC Press, Boca Raton, FL 1983).
2. J. C. ELLIOTT, "*Structure and chemistry of apatites and other calcium orthophosphates*" (Elsevier, Amsterdam, 1994) pp. 34–50.
3. G. HEIMKE and P. GRISS, "*Bioceramics of calcium phosphate*", edited by K. de Groot (CRC Press, Boca Raton, FL 1983) pp. 79–97.
4. P. VIEILLARD and Y. TARDY, in "*Phosphate minerals*", edited by J. O. Nriagu and P. B. Moore (Springer, Verlag, Berlin, 1984) pp. 171–198.
5. J. ANDO, *Bull. Chem. Soc. Jpn.* **31** (1956) 196.
6. H. MONMA, *MRS Int. Meet. Adv. Mater.* **13** (1989) 15.
7. A. A. MIRTCHI, J. LEMAITRE and N. TERAO, *Biomaterials* **10** (1989) 475.
8. M. BOHNER, J. LEMAITRE and T. A. RING, in "*Third Euro-Ceramics*", edited by F. Duran and J. F. Fernandez, Faeza Editrice Iberica) **3** (1993) 95.
9. M. BOHNER, Thesis n° 1171, Ecole Polytechnique Fédérale de Lausanne (Switzerland) 1993.
10. M. MATHEW, L. W. SCHROEDER, B. DICKENS and W. E. BROWN, *Acta Crystallogr.* **B33** (1977) 1325.
11. B. DICKENS, L. W. SCHROEDER and W. E. BROWN, *J. Solid State Chem.* **10** (1974) 232.
12. M. A. BREDIG, H. H. FRANCK and H. FÜLNDER, *Zeitschr. Elektrochem.* **39** (1933) 959.
13. E. D. EANES, *Calcif. Tissue Res.* **5** (1970) 33.
14. T. KANAZAWA, T. UMEGAKI and N. UCHIYAMA, *J. Chem. Technol. Biotechnol.* **32** (1982) 399.
15. A. MORTIER, J. LEMAITRE and P. G. ROUXHET, *Thermochim. Acta* **113** (1979) 133.
16. A. MORTIER, J. LEMAITRE and P. G. ROUXHET, *ibid.* **143** (1989) 143.
17. J. H. WELCH and W. GUTT, *J. Chem. Soc.* (1961) 4442.
18. G. TRÖMEL, H. J. HARKORT and W. HOTOP, *Zeitschr. Anorg. Chem.* **256** (1948) 253.
19. R. W. NURSE, J. H. WELCH and W. GUTT, *J. Chem. Soc.* (1959) 1077.
20. J. ANDO, *Bull. Chem. Soc. Jpn.* **31** (1958) 201.
21. J. L. MIQUEL, L. FACCHINI, A. P. LEGRAND, X. MARCHANDISE, P. LECOUFFE, M. CHAVANAZ, M. DONAZZAN, C. REY and J. LEMAITRE, *Clin. Mater.* **5** (1990) 115.
22. D. C. MONTGOMERY, in "Design and analysis of experiments", 3rd Edn (John Wiley & Sons, New York, 1991) pp. 335–386.

Received 16 June
and accepted 7 September 1995